Evolution of Interannual Warm and Cold Events in the Southeast Atlantic Ocean

P. FLORENCHIE, C. J. C. REASON, J. R. E. LUTJEHARMS, AND M. ROUAULT

Department of Oceanography, University of Cape Town, Rondebosch, South Africa

C. ROY

Institut de Recherche et Developpement, Paris, France

S. MASSON

Frontier Research System for Global Change, Kanagawa, Japan

ABSTRACT

Extreme warm episodes in the southeast Atlantic Ocean, known as Benguela Niños, have devastating environmental impacts and have been shown to be remotely forced. To place these extreme events into perspective, the investigation is here extended to minor warm events as well as to cold episodes. To this end, different sets of observations have been combined with outputs from a numerical simulation of the tropical Atlantic for the period 1982–99. It is shown that both warm and cold surface events develop regularly in the same specific region along the coast of Angola and Namibia. Some cold events compete in magnitude with major warm episodes. Local sea–air heat flux exchanges do not seem to precondition the sea surface in the Angola–Benguela region prior to the arrival of an event. Most warm and cold episodes are large-scale events despite their limited surface signature. They appear to be generated by wind anomalies in the western and central equatorial Atlantic in the same way as Benguela Niños. Seasonal fluctuations of the depth and shape of the tropical thermocline seem partly to control the way subsurface anomalies eventually impact the surface. During austral summer, surface anomalies create an identifiable pool centered near 15°S, whereas in winter they show an elongated pattern along the coast stretching toward the equator. Local upwelling or downwelling favorable wind regimes, as well as local net heat fluxes, may modulate the surface expression of events.

1. Introduction

Benguela Niños are intermittent, acute, extreme warm events near the border between the southward-flowing Angola Current and the Benguela upwelling system off southwestern Africa (Shannon et al. 1986). These anomalously warm events have dramatic effects on the fisheries and the climate of the region. They tend to induce significant rainfall anomalies (Rouault et al. 2003) and can drastically modify fish distribution and abundance (Boyer et al. 2001). The collapse of the Namibian sardine stock after 1974 followed a protracted warm event during 1972–74, the effect of which was aggravated by overfishing (Boyer and Hampton 2001). More recently, the 1995 event had a drastic impact on the whole ecosystem with a 4°–5° southward shift of the sardine population, associated with high mortality and poor recruitment of the major pelagic fish species (Boyer and

Hampton 2001). In essence, Benguela Niños express themselves as abnormally and persistent high sea surface temperatures (SST) along the coast of Angola and Namibia.

According to many authors the equatorial interannual variability pattern in the Atlantic is similar to the ENSO phenomenon in the Pacific, but is weaker and not self-sustained (Sutton et al. 2000; Chang et al. 2000; Servain et al. 1999; Zebiak 1993). Benguela Niños occurred in 1934, 1949, 1963, 1984 (Shannon et al. 1986) and more recently in 1995 (Gammelsrød et al. 1998). Such episodes are less frequent and less intense than their Pacific counterparts, and they tend to develop south of the equator. To explain the origin of climate anomalies in the eastern tropical Atlantic, Hirst and Hastenrath (1983) suggested a causality chain of atmospheric–oceanic anomalies across the basin. Rather than being locally forced by wind anomalies, equatorial warm anomalies could be linked to a relaxation of zonal wind stress in the western equatorial Atlantic, as shown by Delecluse et al. (1994) in a study of the 1984 event based on a simulation of the tropical Atlantic Ocean. Florenchie et

Corresponding author address: Dr. Chris Reason, Department of Oceanography, University of Cape Town, Rondebosch 7701, South Africa.
E-mail: cjr@egs.uct.ac.za

al. (2003) demonstrate that the 1984 and 1995 Benguela Niños originated as temperature anomalies on the tropical/equatorial thermocline, propagated zonally from there, turned south on reaching the west African coastline, and outcrop only on reaching a specific area, called the Angola–Benguela frontal zone (Meeuwis and Lutjeharms 1990). In this paper, we extend the Florenchie et al. (2003) study by using a combination of an ocean general circulation model and satellite-derived observations of sea surface temperature, sea surface height (SSH), wind stress, and surface heat flux to further investigate the propagation mechanism of Benguela Niños in more detail, and also by considering cold events as well as other warm events in the southeast Atlantic.

Picaut (1985) suggested that eastern tropical oceans are primarily governed by remote wind stress effects through equatorial wave dynamics. Anomalies in the trade winds may trigger Kelvin waves that subsequently propagate eastward along the equator, inducing a deepening or a lifting of the thermocline. At the surface, Kelvin waves may be detected by their sea level signature and their phase speed, of the order of 2 m s^{-1}. Thus, it is possible that equatorial Kelvin waves may play a role in the evolution of Benguela Niños. In this study, we explore the development and propagation of anomalies across the equatorial Atlantic Ocean and their ability to create a variety of sea surface temperature anomalies on the southeastern side of the basin, that is, the shelf region off Angola and Namibia.

There are also links between ENSO and the equatorial and tropical North Atlantic via atmospheric teleconnections (Delecluse et al. 1994). In a modeling study, Saravanan and Chang (2000) have described a surface wind stress signal over the western equatorial Atlantic associated with ENSO. Latif and Barnett (1995) found that the dominant response in the Atlantic to ENSO is a lowering of SST in the equatorial area. The observational analyses of Enfield and Mayer (1997) suggest that the mean easterly winds are intensified in the western equatorial Atlantic in response to Pacific warm events but that coherent local changes in SST are less obvious. However, in the upwelling zone off West Africa (10°–24°N), a coherent ENSO signal in winds and SST was found by Roy and Reason (2001). Curtis and Hastenrath (1995) concluded that warm events in the Pacific induce only a modest warming in the western tropical Atlantic whereas Ruiz-Barradas et al. (2000) and Zebiak (1993) found no significant impact of ENSO on the Atlantic Niños (equatorial Atlantic Ocean variability). In the South Atlantic, composite maps of SST and wind anomalies derived for 14 strong events during the past century (Reason et al. 2000) suggest that warm (cool) anomalies evolve in certain large areas of the subtropical/midlatitude southeast Atlantic during the transition and peak phases of El Niño (La Niña) in association with stronger (weaker) trade winds. Taken together, this previous work suggests that there is an ENSO impact in the eastern Atlantic but the exact relationship between

this signal and other modes such as Benguela Niños and cold events remains to be clarified.

Other minor warm (1986, 1988) and cold events (1969, 1982/83) in the southeast Atlantic have been partly documented (Carton and Huang 1994; Walker 1987; Boyd et al. 1987). It appears from the various studies cited earlier that the distinction between Benguela Niños and other warm events is not always clear and that a quantitative definition of warm or cold events is still missing. This study intends to clarify the differences between Benguela Niños and other warm events and to provide a description of cold events as well.

To investigate the origin and the vertical structure of each episode, various sets of observations (sea surface temperature, sea level and wind anomalies, surface heat flux anomalies) are used together with Océan Parallélisé (OPA) ocean general circulation model simulations (Madec et al. 1999) of the tropical Atlantic Ocean. All warm and cold events that occurred in the southeast Atlantic from 1982 to 1999 are described and analyzed with a special attention given to the major ones. An additional motivation for this work is to assess the possibility of forecasting such events, particularly the extreme cases, on an operational basis. Hence this investigation addresses the following questions:

- what are the spatial and temporal scales of warm and cold events in the southeast Atlantic?
- what are the underlying mechanisms driving the various events?
- how do Benguela Niños differ from other warm events?
- are these warm and cold events predictable?

In section 2, sea surface temperature data are analyzed to assess the location, frequency, duration, and spatial coverage of the surface manifestation of various warm and cold events occurring in the eastern Atlantic. In sections 3 and 4 observed sea level and wind anomalies recorded during various events are described. Section 5 deals with sea–air heat flux exchanges. In section 6, model outputs are compared to observations and studied at different depths to understand the origin of the different anomalies and their vertical structures.

2. Observations over the last 20 yr from sea surface temperature

a. Standard deviation of SST and SST anomalies

Monthly maps of optimal interpolated sea surface temperature (OI-SST) with a horizontal resolution of 1° are analyzed from November 1981 to December 2000. OI-SST data are a blend of satellite and in situ observations (Reynolds and Smith 1994). Optimal interpolated sea surface temperature anomalies (OI-SSTA) are extracted from OI-SST data by calculating a monthly climatology from 1982 to 1999, the period also covered by the model simulations. Then standard deviation
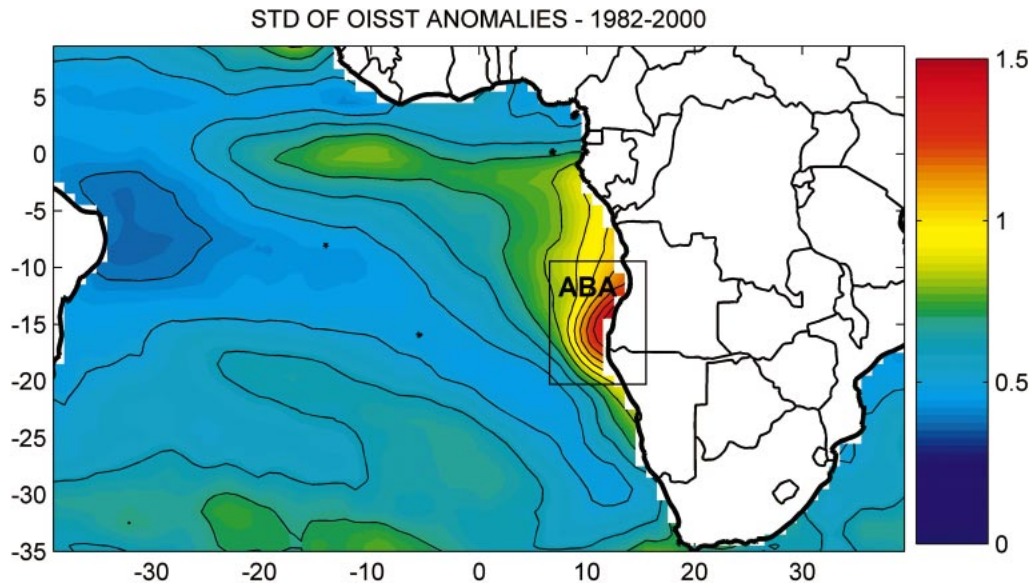
FIG. 1. Standard deviation of OI-SST anomalies over the South Atlantic Ocean (°C).

(STD) is used to depict the main areas of OI-SSTA interannual variability over the tropical South Atlantic basin.

High levels of SSTA standard deviation concentrate in the eastern Atlantic, spreading roughly from the equator to 20°S and from 5°E to the African coast (Fig. 1). This area corresponds also to the area with the largest seasonal signal amplitude (not shown) although the range of interannual variability remains smaller compared to the seasonal one, as already noted by Servain and Arnault (1995). A local maximum of variability appears in a specific area between 10° and 20°S and from 8°E to the continent, hereafter to be called the ABA (Angola–Benguela area). The ABA includes the Angola–Benguela frontal zone (ABFZ), where warm water from the equator flows poleward along the coast in the Angola Current and meets the much cooler water from the northwestward Benguela Current (Shannon et al. 1987; Meeuwis and Lutjeharms 1990). The front represents a transition zone between the more tropical ecosystem in the north and the upwelling-driven ecosystem in the south and its average latitude is about 15°S (Lass et al. 2000). Meridional movements of the front could be responsible for the strong SST anomalies in the ABA region. During Benguela Niños, it tends to be displaced southward following an intrusion of warm and saline water of equatorial origin as far as 25°S (Mohrholz et al. 2001; Shannon et al. 1986).

The interannual variability appears to show seasonality with a pronounced maximum in March/April limited to the ABA and in phase with late summer warming. In June/July, variability levels are much lower while their spatial coverage increases and spreads equatorward. Typically, the amplitude of SST anomalies reaches a minimum in the ABA in September/October with values close to zero. Conversely, interannual variability is found to be higher during austral winter north of the ABA in the eastern equatorial Atlantic Ocean, as already shown by Carton and Huang (1994) in their study based on a 28-yr record.

b. Identification of various warm and cold events

Time series of OI-SST and OI-SSTA, averaged over the ABA area (19.5°–10.5°S and 8.5°–15.5°E), form an index that we use to assess the periodicity, magnitude, and duration of anomalies over the 1982–2000 period. During this period, the 1984 and 1995 Benguela Niños were the most intense warm episodes over the ABA while pronounced cool events occurred in 1982, 1983, and 1997 (Fig. 2). SST anomalies were large during these events, exceeding 3°C (e.g., 1982, 1984) and 5°C (1995) in certain areas. The 1984 and 1995 Benguela Niños occurred in phase with late summer (March/April), thereby inducing very high SST magnitudes in the ABA.

Shannon et al. (1986) and Walker (1987) suggested that Benguela Niños have a periodicity of about 10 yr. The low-frequency components embedded in the OI-SSTA signal were investigated using the continuous wavelet transform of Torrence and Compo (1998). This analysis showed that the main component has a period of 18 months with maximum amplitude from 1982 to 1986 and from 1994 to 1997; both periods include at least one cold event and a Benguela Niño. This corresponds to an amplitude modulation of the 18 months period of about 12 yr, but Fig. 2 reveals that significant warm and cold episodes developed at various times during the period of study with a succession of warm peaks after 1997.

OISST ANOMALIES - ANGOLA/BENGUELA AREA (ABA)
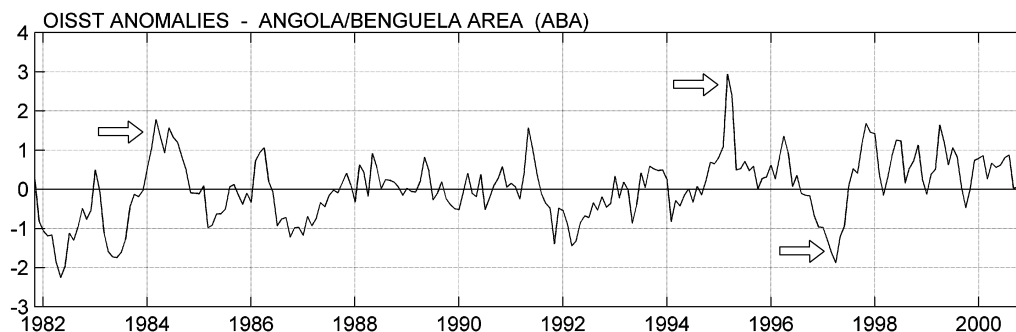
FIG. 2. Time series of OI-SSTA averaged over the ABA (°C).

By considering only spatially averaged anomalies in the ABA exceeding 1°C, one can identify a series of warm events (including the two Benguela Niños) in 1984, 1986, 1991, 1995, 1996, 1997/98, and 1999 and five cold events in 1982, 1983, 1986/87, 1991/92, and 1997. The 1982, 1983, and 1997 negative anomalies are similar in magnitude to the positive ones observed in 1984. Many events reach a maximum of intensity in March/April (1984, 1986, 1995, 1996, 1997, and 1999) following the seasonality in the interannual variability mentioned earlier. Nevertheless, other events reached a maximum between May and July (1982, 1983, second peak of 1984, 1991, and 1998) or later in the year (1997/98). The duration of the events varies from a few months (1986, 1991, 1995, 1996, 1997/98, 1998, and 1999) to 6 months or more (1982, 1983, 1984, 1986/87, 1991/92, and 1997). On average, cold episodes at the surface seem to last longer than their warm counterparts.

Figure 3 depicts a time series of OI-SST climatology averaged over the ABA (gray) and superimposed with OI-SST (black). This figure emphasizes the importance of the season; warm events developing in phase with late summer (March–April) will induce very high SST in the ABA as observed in 1984 and 1995 and to a certain extent in 1986, 1996, and 1999. By contrast, the short 1991 warm event reached its peak in May and SSTs remained below the climatological mean of March/April. The cold 1997 event stands out as the coolest in terms of magnitude of absolute SST during summer.

Although simple, the following argument might help to understand why not all warm events have a strong impact on biota and climate. First, intense warm events occurring during summer may elevate temperature above the viable temperature range of marine organisms. Secondly, the second half of summer (January–April) tends to be the season of maximum rainfall over northern Namibia and southern Angola. Southeastern Atlantic SSTs influence the atmospheric moisture and stability in the region (Hirst and Hastenrath 1983). As a result, anomalous episodes reaching maturity in March/April are likely to have an impact on rainfall; cold events in phase with summer (like the 1997 one) may induce dry seasons while warm events may be associated with wetter rainy seasons. Rouault et al. (2003) have examined atmospheric moisture fluxes over the region during four recent warm events and suggested that the relation of these fluxes to the mean atmospheric transport and the location of the warm SST anomaly may also play a key role. In general, each event (warm or cold) appears to have a specific impact on regional fisheries and rainfall, whose magnitude depends on a combination of different factors: surface coverage, intensity, duration, and period of maximum intensity during the year.

Spatial coverage of the anomalies shows a seasonal trend that could be linked to the seasonal fluctuation of the thermocline. For example, they tend to be limited to the ABA in March/April showing an intense and specific pattern at that time but tend to extend farther

OISST (B) - OISST CLIM (G) - ANGOLA/BENGUELA AREA
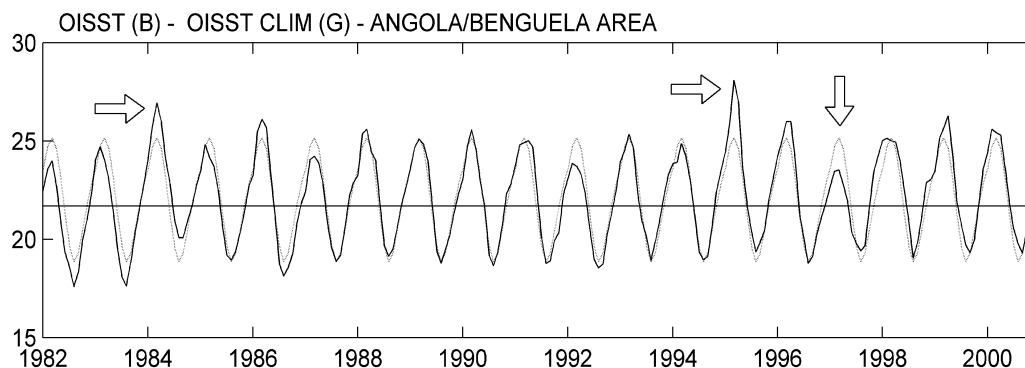
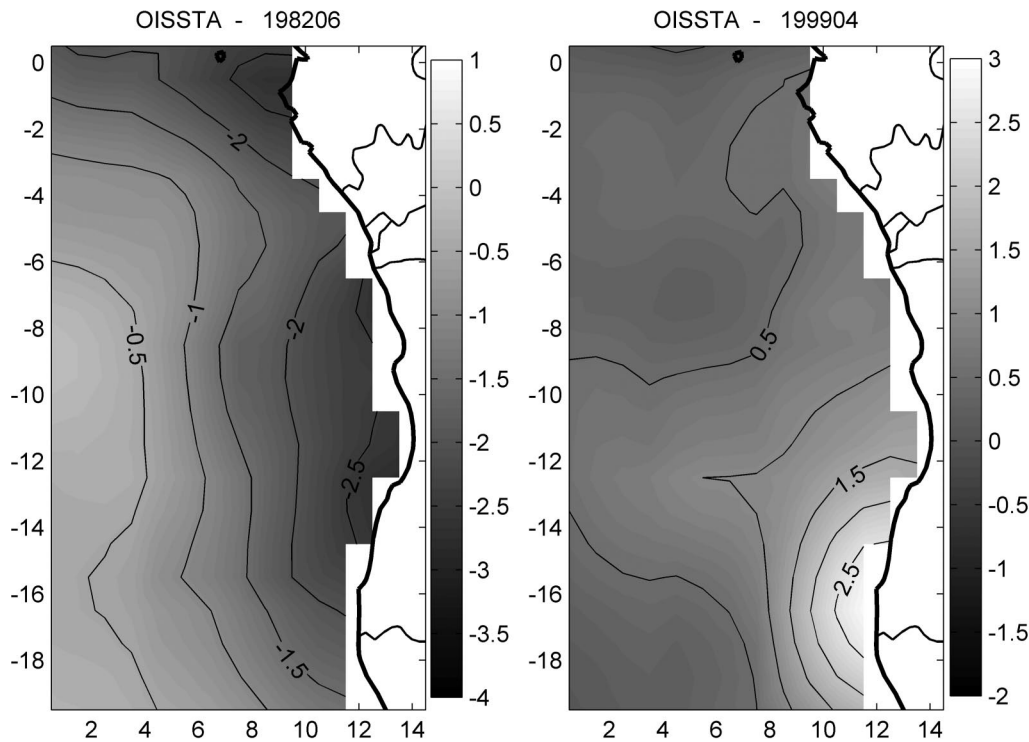FIG. 3. Time series of OI-SST (black) and OI-SST climatology (gray) averaged over the ABA (°C).

FIG. 4. Surface expressions of OI-SSTA in Jun 1982 and in Apr 1999 (°C).

north in winter. Figure 4 illustrates two typical patterns encountered in June 1982 and in April 1999. The main upwelling period north of 25°S extends from about March to November peaking around August (Shannon et al. 1986). Since Ekman suction implies an elevation of the thermocline toward the surface along the coast, SSTs here may become more sensitive to additional vertical shifts of the thermocline, for instance, under the action of upwelling coastal trapped waves. By contrast, permanent upwelling in the eastern Pacific makes subsurface temperature anomalies visible at the surface near the equator. In an observational study, Shannon et al. (1987) found the thermocline lying off Angola at a depth of around 25 m and extending southward to the Angola–Benguela front around 16°S where it seemed to outcrop. North of 16°S, vertical stratification is more intense during summer with a marked thermocline while in the frontal area, horizontal stratification is weaker during winter (Shannon et al. 1987, their Fig. 7). As a result, coastal temperature anomalies associated with thermocline shifts in summer might remain below the surface north of the front but reach it as they approach the front, thereby creating an intense anomaly pool.

3. TOPEX/Poseidon sea level anomalies versus OI-SSTA

Satellite TOPEX/Poseidon sea level (SL) measurements used here cover the period from 1992 to 2000 with a 5-day temporal resolution and a 1° spatial res-

olution. Shannon et al. (1986) have indicated that Benguela Niños are characterized by a rise of sea level of several centimeters. Monthly TOPEX/Poseidon sea level anomalies (SLA) have been computed over the South Atlantic from October 1992 to January 2001 to identify the signature of each event in terms of sea level anomaly.

SLA and OI-SSTA variability present a similar spatial pattern with high values concentrated along the African coast in the eastern basin (Fig. 5). However the highest level of SLA variability occurs in an area north of the ABA roughly between the equator and 5°S. SLA variability along the coast also shows a seasonal trend with high values from January to April and a maximum in March centered near 3°S (not shown). Sea level anomalies seem to propagate along the coast from March to April. The location of maxima near the equator suggests that equatorial wave-type disturbances are responsible.

To consider the evolution of the events, Fig. 6 shows sea level (right) and sea surface temperature (left) anomalies along the African coast from the equator to 30°S versus time. All warm (cold) episodes over the 1992–2000 period tend to be associated with positive (negative) sea level anomalies spreading along the coast from the equator to as far south as about 20°S. The 1995 and 1996 warm events show positive anomalies with respective local maxima of 12 and 10 cm, while the 1997 cold event shows strong negative anomalies with a local minimum of −11 cm. We can also distinguish the series of positive peaks in 1997/98, 1998, and 1999 corre-

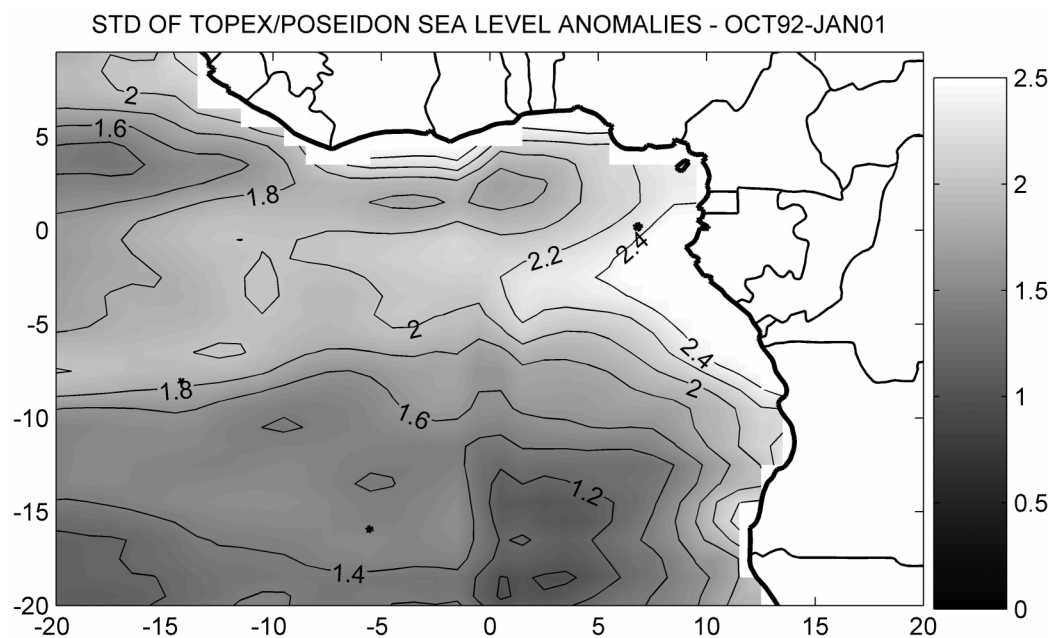STD OF TOPEX/POSEIDON SEA LEVEL ANOMALIES - OCT92-JAN01

FIG. 5. Standard deviation of TOPEX/Poseidon sea level anomalies (cm).

sponding to the three warm episodes. Equatorial sea level anomalies tend to propagate southward along the coast as can be seen in Fig. 6b, especially during the 1997 and the 1999 events. Calculations from the slope of these plots suggest a poleward propagation rate of between 0.5 and 1 m s^{-1}. Such an estimate agrees with the poleward propagations observed in the eastern Pacific by Enfield and Allen (1980) or simulated (Clarke
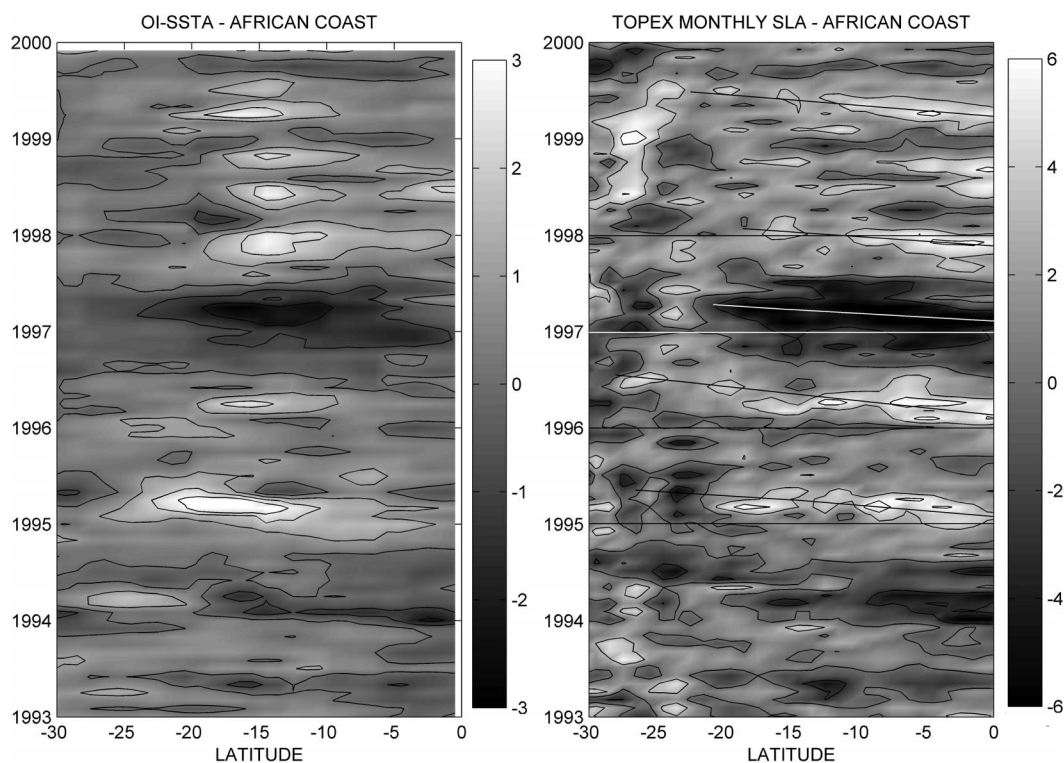
OI-SSTA - AFRICAN COAST   TOPEX MONTHLY SLA - AFRICAN COAST

FIG. 6. (left) Sea surface temperature and (right) sea level anomalies along the African coast from the equator to 30°S vs time (units are °C and cm).
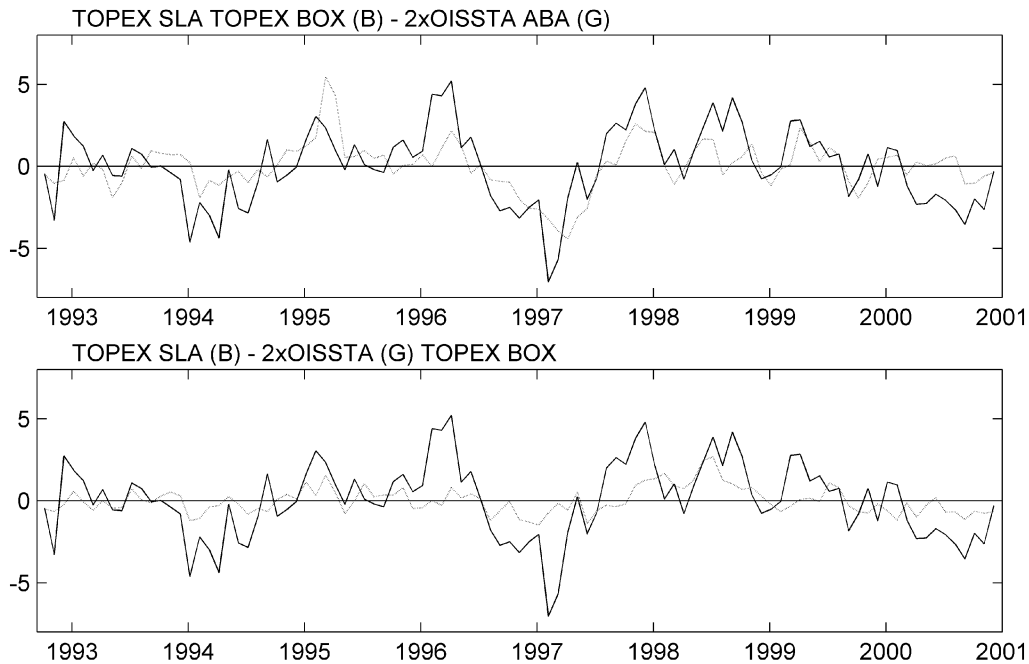
FIG. 7. (a) Time series of SLA (black) and OI-SSTA (gray) averaged, respectively, on the T/P box and the ABA. (b) Time series of SLA (black) and OI-SSTA (gray) averaged on the T/P box (units are cm and °C).

and Van Gorder 1994). A coastal trapped wave propagation process is consistent with the spreading of anomalies from the equator southward. However, discrepancies between theoretical phase speeds and the slower observed ones may occur because the theory does not take into account coastal shelf and slope bottom topography or bottom friction (Clarke and Van Gorder 1994; Pizarro et al. 2001).

In Fig. 7a, we have superimposed time series of OI-SSTA (gray) and SLA (black) averaged, respectively, over the ABA and over a limited equatorial area hereafter called the TOPEX/Poseidon (T/P) box (2.5°S–2.5°N, 5.5°–10.5°E). In Fig. 7b, both time series are averaged over the T/P box. In Fig. 7a, the two time series are correlated with a maximum coefficient of 0.67 with a 1-month lag in favor of the T/P signal, thus supporting an equatorial origin of most episodes over this period. The OI-SSTA signal in Fig. 7b is very weak because the events tend to propagate along the thermocline and the surface expression is weak along the equator; however, the events can be easily recognized via the sea level anomalies. In January 1995, sea level positive anomalies can be observed propagating eastward along the equator from about 40°W to the African coast with an average speed of 150 km day^{-1}, in good agreement with the theoretical phase speed of Kelvin waves (2 m s^{-1}). To determine the remote or local forcing generating these sea level anomalies (and subsequently the SST anomalies over the ABA), we have used *European Remote-Sensing Satellite-1* (*ERS-1*) and *-2* (*ERS-2*) satellite wind speed observations over the period 1992–2000.

4. ERS wind speed anomalies versus T/P SLA and OI-SSTA

ERS-1 and *ERS-2* zonal and meridional monthly wind speed anomalies (WSA) available on a 1° spatial grid have been analyzed over the period 1991–2000. By contrast with sea level or SST, seasonal and interannual zonal wind variability show opposite spatial patterns with low values in the eastern equatorial Atlantic and high levels west of 20°W (not shown). Zonal WSA have been averaged respectively over different areas and compared to sea level anomalies averaged on the T/P box. The best correlation between the two signals is obtained when zonal WSA are averaged on an area south of the equator (between 5.5°S and 0.5°N) in the western central basin from 29.5° to 19.5°W with a maximum correlation of 0.60 and a lag shorter than 1 month for the wind (Fig. 8a). The two signals are no longer correlated when zonal WSA are averaged in the eastern equatorial basin or north of the equator (not shown). Figure 8b reproduces similar time series between the WSA averaged in the south-central equatorial basin and the OI-SSTA averaged over the ABA. Maximum correlation is now 0.55 with a 1-month lag in favor of the wind.

Figure 8a suggests that the eastern equatorial Atlantic is directly influenced by remote zonal wind stress anomalies through equatorial wave dynamics (there is less than a 1-month lag between the two signals). As noted by Picaut (1985), equatorial oceans tend to respond clearly and coherently to wind fluctuations as seems to be the case here. Anomalies in the trades in the western
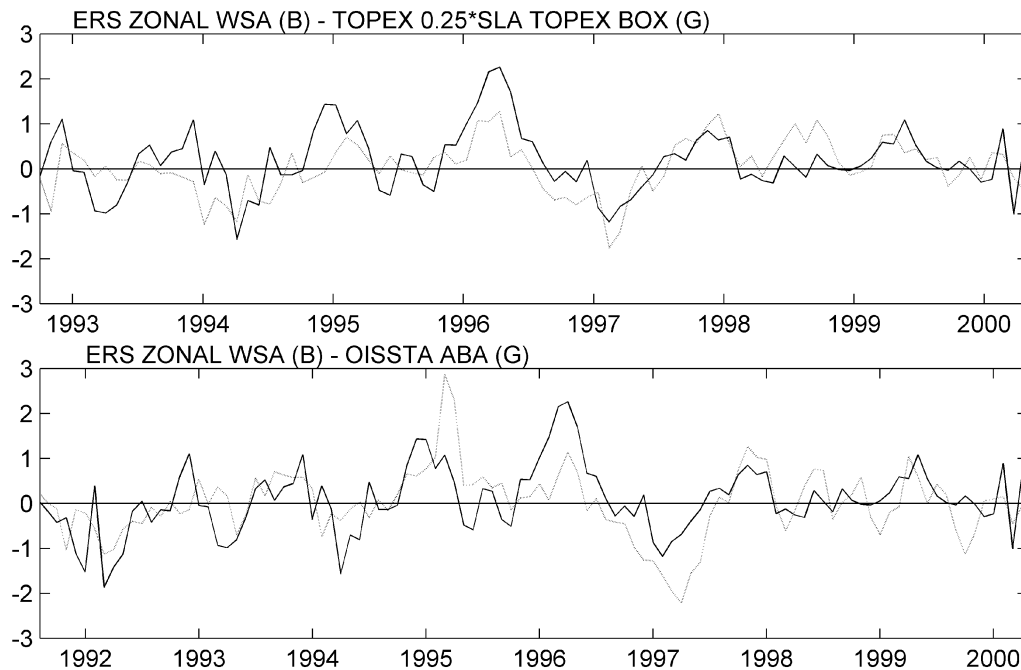
FIG. 8. Time series of zonal WSA averaged south of the equator (between 5.5°S and 0.5°N, black) in the central basin from 29.5° to 19.5°W and (a) SLA averaged over the T/P box (gray) and (b) OI-SSTA averaged over the ABA (gray) (units are cm s⁻¹, cm, and °C).

to central equatorial basin excite eastward-propagating Kelvin waves that depress or lift the thermocline all the way to the African coast and create subsurface temperature anomalies. On reaching the African coast, coastal trapped waves are generated which propagate southward and induce SSTA in the ABA, where the thermocline reaches the surface. As mentioned earlier, the shape and depth of the thermocline as well as the local wind regime may modify the surface expression of the anomalies. Figure 8b tends to confirm such a scenario. The 1995, 1996, and 1997/98 warm events could be associated with a diminution of westward zonal winds (positive anomalies) through downwelling equatorial waves while the 1997 cold event could be a response to an increase of trade winds over the same large area via upwelling equatorial waves. Zonal and meridional wind anomalies in the eastern equatorial Atlantic and/or north of the equator show much weaker correlation with SSTA or SLA over the ABA and the eastern equatorial area.

We also note that the response in terms of SSTA in the ABA to the remote wind forcing is not linear. For example, the weak 1996 warm event is associated with stronger sea level and zonal wind anomalies along the equator than the 1995 warm and 1997 cold events. This observation poses challenges for forecasting the strength of the events. SST anomalies in the ABA appear to be potentially predictable but factors like local wind regimes, heat flux anomalies, coupling between the atmosphere and the ocean with subsequent positive or negative feedbacks may play a key role in controlling the evolution of each event.

5. Ocean–atmosphere flux exchanges

In this section, we consider whether the anomalies described here may have been contributed to by local air–sea heat flux exchanges as well as by ocean dynamical processes. To address this aspect, we have carried out an analysis of sea surface heat fluxes from the National Centers for Environmental Prediction–National Center for Atmospheric Research (NCEP–NCAR) 40-year Reanalysis (Kalnay et al. 1996) over the South Atlantic Ocean. Net heat flux anomalies have been computed over the period 1980–2000. First, the correlation between OI-SST anomalies averaged over the ABA and net heat flux anomalies has been calculated at each point over the entire basin. It shows that the correlation reaches a maximum over the ABA, with a maximum value of about 0.68 and a lag of about 1 month in favor of SST anomalies. It is worth noting that most of the interannual variability of the net surface heat flux occurs in an area well to the northwest of the ABA. The latent heat flux is the main contributor to the surface heat flux variability over the tropical southeast Atlantic Ocean. However, it appears that anomalies in the net heat flux over this area are weakly correlated with SST anomalies over the ABA, with values below 0.35. Figure 9 illustrates the time series of SST and net surface heat flux anomalies averaged over the ABA. Positive anomalies
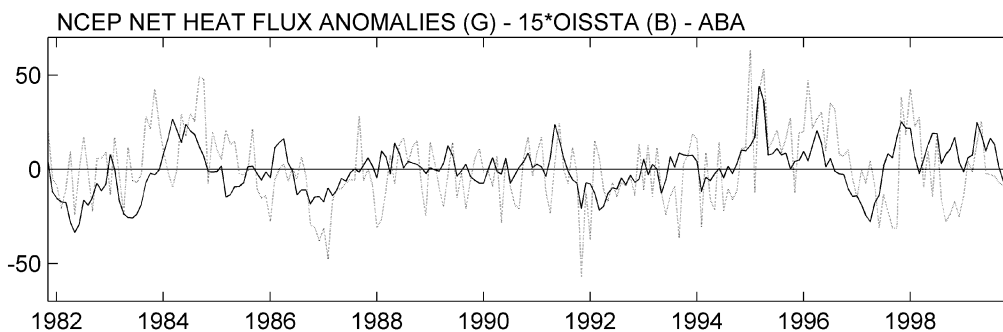
NCEP NET HEAT FLUX ANOMALIES (G) - 15*OISSTA (B) - ABA

FIG. 9. Time series of NCEP net heat flux (gray) and OI-SST (black) anomalies averaged over the ABA (units are W m^{-2} and °C).

of the flux correspond to a net heat loss for the ocean. The comparison between the two signals reveals that net surface heat flux anomalies do not precondition the sea surface in the ABA. It shows that during all warm events, the ocean loses heat. Maximum flux anomalies of about 60 W m^{-2} occurred during the 1984, 1995, and 1998 major events. Likewise, during cold events, the flux anomalies are opposite, with maximum values of heat gain into the ocean of between 20 and 40 W m^{-2}. On a seasonal basis, the ocean heat gain is maximum from October to December with a net heat flux of about 90 W m^{-2} and reaches a minimum value of about 20 W m^{-2} in June over the ABA. In March/April, the mean net heat flux is about 70 W m^{-2} toward the ocean. Hence, warm and cold events induce strong heat anomalies in comparison to the annual cycle. In conclusion, local net heat flux seems to have a rather passive role, acting as a thermostat to regulate cold and warm events at the surface, mainly via latent heat flux anomalies.

6. Model simulation—1979–99

In order to investigate the vertical and horizontal structures of the temperature anomalies below the surface, we have studied outputs from a tropical ocean model, the OPA version 8 OGCM developed at Laboratoire d'Océanographie Dynamique et de Climatologie (LODYC; Madec et al. 1999). This version of OPA solves the primitive equations assuming the Boussinesq and hydrostatic approximations, the incompressibility hypothesis and the use of a rigid-lid boundary at the sea surface. Simulations were performed at LODYC with the Three Tropical Ocean Configuration (TOTEM) in which the grid has a relatively high resolution (0.33° maximum near the equator in the zonal and meridional directions) covering the oceans between 45°S and 45°N. The vertical grid has 30 levels and a resolution of 10 m from the surface to 150 m, which decreases significantly after 600 m. There is no restoring term in temperature and salinity between 20°S and 20°N. Outside of this belt, a linear restoring term is applied towards the monthly mean temperature and the seasonal salinity fields of Levitus (1982).

This restoring term is applied only under the mixing layer with a time constant decreasing from 250 days at 20° to 30 days along the northern and southern boundaries of the domain. The Brunt–Väisälä frequency is used to compute the turbulent kinetic energy (TKE; Blanke and Delecluse 1993), which determines the vertical mixing coefficients. In this simulation, the freshwater flux is introduced as a pseudosalt flux. It is prescribed as a boundary condition on vertical diffusion flux of salinity. To avoid unrealistic temperature drift induced by the heat forcing biases and model deficiencies, a relaxation of SSTs of the first layer at 5 m toward observed SSTs is added to the European Centre for Medium-Range Weather Forecasts (ECMWF) heat flux. A complete description of this model is available in Maes et al. (1998).

The model is forced by daily wind stress, net surface solar radiation, net surface heat flux, and net freshwater flux (evaporation minus precipitation). Except for the net freshwater flux, these fields are taken from the ECMWF Re-Analysis (1979–91), (ERA-15; Gilson et al. 1999). Comparisons of the ERA-15 precipitation with different climatologies led to the choice of Climate Prediction Center (CPC) Merged Analysis of Precipitation (CMAP) precipitation (Xie and Arkin 1998) for the freshwater flux boundary condition (Masson et al. 2002). Evaporation, linked to the latent heat flux, is taken from ERA-15. From 1992, ERS wind stress data are used instead of ERA-15 and from 1994 heat forcing fluxes and the evaporation are extracted from ECMWF analyses.

We have used the monthly model outputs to study temperature anomalies over the period 1979–99 at different depths in the upper ocean (5, 25, 45, 75, and 100 m). A climatology has been calculated over the 1982–99 period to match the climatology of the OI-SST observations. Then the model SST anomalies have been extracted, detrended, and compared to OI-SST anomalies. It is important to emphasize than the model SST fields are influenced via a relaxation term toward observed SST in the air–sea heat budget equation. Hence it is expected that the model near-surface temperatures
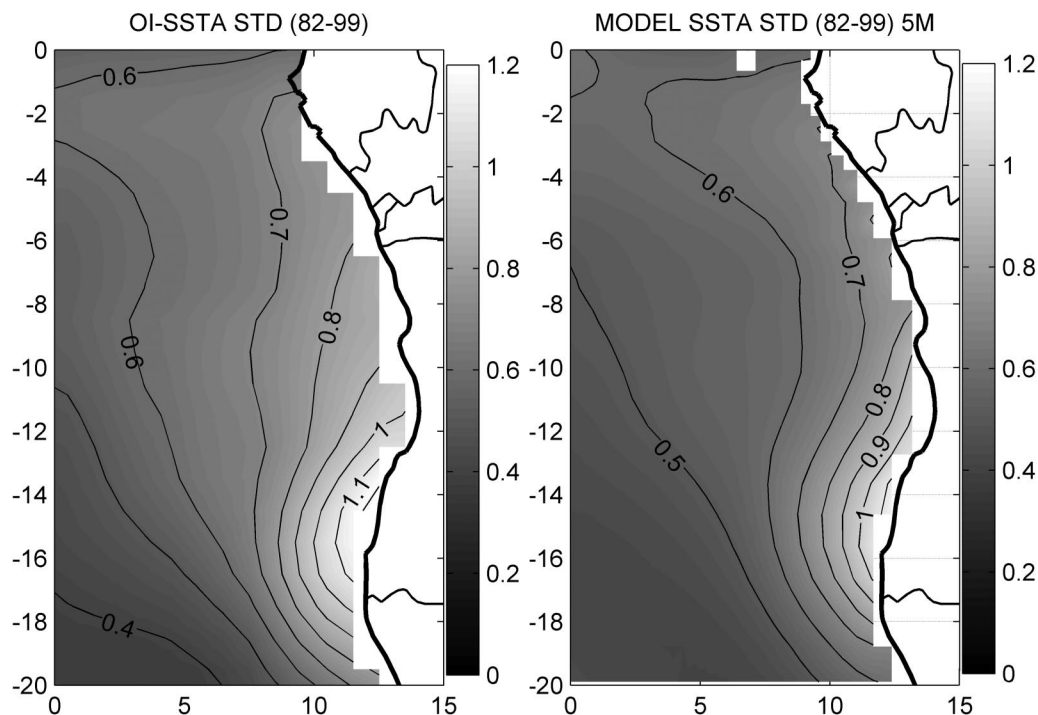
FIG. 10. Standard deviation of (left) OI-SSTA and (right) model SSTA (°C).

will be in rather good agreement with Reynolds SST data.

a. Comparison between model monthly SSTA and OI-SSTA

Figure 10 shows standard deviations of model temperature anomalies at 5-m depth and OI-SSTA for the period November 1981–December 1999. The area of highest model SSTA variability corresponds to the one obtained from OI-SSTA (roughly from 20° to 10°S and 8°E to the coast). However, we note that variability levels are underestimated by the model with a mean ratio of 0.81 over the ABA. Monthly model SSTAs have then been spatially averaged on the ABA to build time series for the period 1979–99. A comparison with observations in Fig. 11 confirms the generally lower amplitudes

of anomalies in the model simulation. According to Delecluse et al. (1994), externally forced wind stress anomalies are important for initiating the interannual variability in the tropical Atlantic but this ocean model is able to develop a relatively large coupled response. Coupled atmosphere–ocean feedbacks are missing in this simulation and this absence might explain the lower SSTA variability in the model. We also note that in Fig. 11 the simulation is more realistic from 1993 to 1999, that is, when the model is forced by *ERS-1* and *ERS-2* winds. The error standard deviation between the two signals is 0.43, instead of 0.57 when ECMWF winds are used. Hence wind stress products may also explain the relative discrepancy of variability levels between the model and the observed SSTs.

Nonetheless, the 1982, 1983, 1984, 1991, 1995, 1997, and 1997/98 events are captured by the model and the
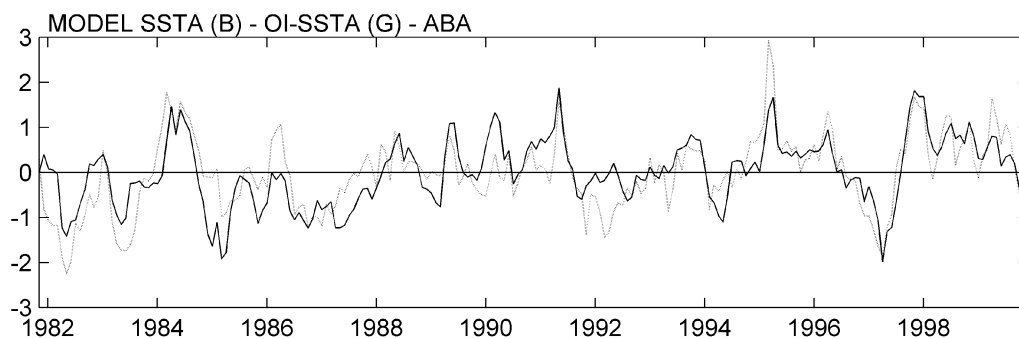

FIG. 11. Time series of model SSTA (black) and OI-SSTA (gray) over the ABA (°C).

FIG. 12. Comparison between (upper row) the monthly OI-SSTA and (lower row) model SSTA in (left) Mar/Apr 1984, (middle) Mar/Apr 1995, and (right) Apr 1997 in the eastern South Atlantic Ocean (°C).

amplitudes of the 1997 and 1997/98 events are realistic. The amplitude of the 1995 episode is significantly underestimated and the duration of the simulated 1984 event is less than the observed one. As a consequence, a lag of about 1 month appears between the real and simulated 1984 peaks. The 1986, 1996, 1998, and 1999 events are not reproduced or show too weak values in the model. In the rest of the paper, we focus on the seven events that are well simulated by the model (1982, 1983, 1984, 1991, 1995, 1997, and 1997/98) with special emphasis on the two Benguela Niños of 1984 and 1995.

Comparison of model monthly SSTA with the OI-SSTA shows that the model reproduces the spatial distribution of the various anomalous patterns along the coast quite well. Figure 12 depicts the mature phase of

three extreme events (1984 and 1995 warm events and 1997 cold event). We show anomalies averaged over March and April to take into account the lag between the simulated and observed 1984 and 1995 peaks. As already mentioned, the 1984 and 1995 model events underestimate the observed amplitude (note that the temperature bar is different for each model plot). These three events reach their mature phase in March/April and April.

b. Model anomalies at different depths in the ABA

Figure 13 represents the spatial coverage of the monthly simulated anomalies at 25-, 45-, 75-, and 100-m depths in March/April when the 1995 Benguela Niño reached its maximum of intensity at the surface.
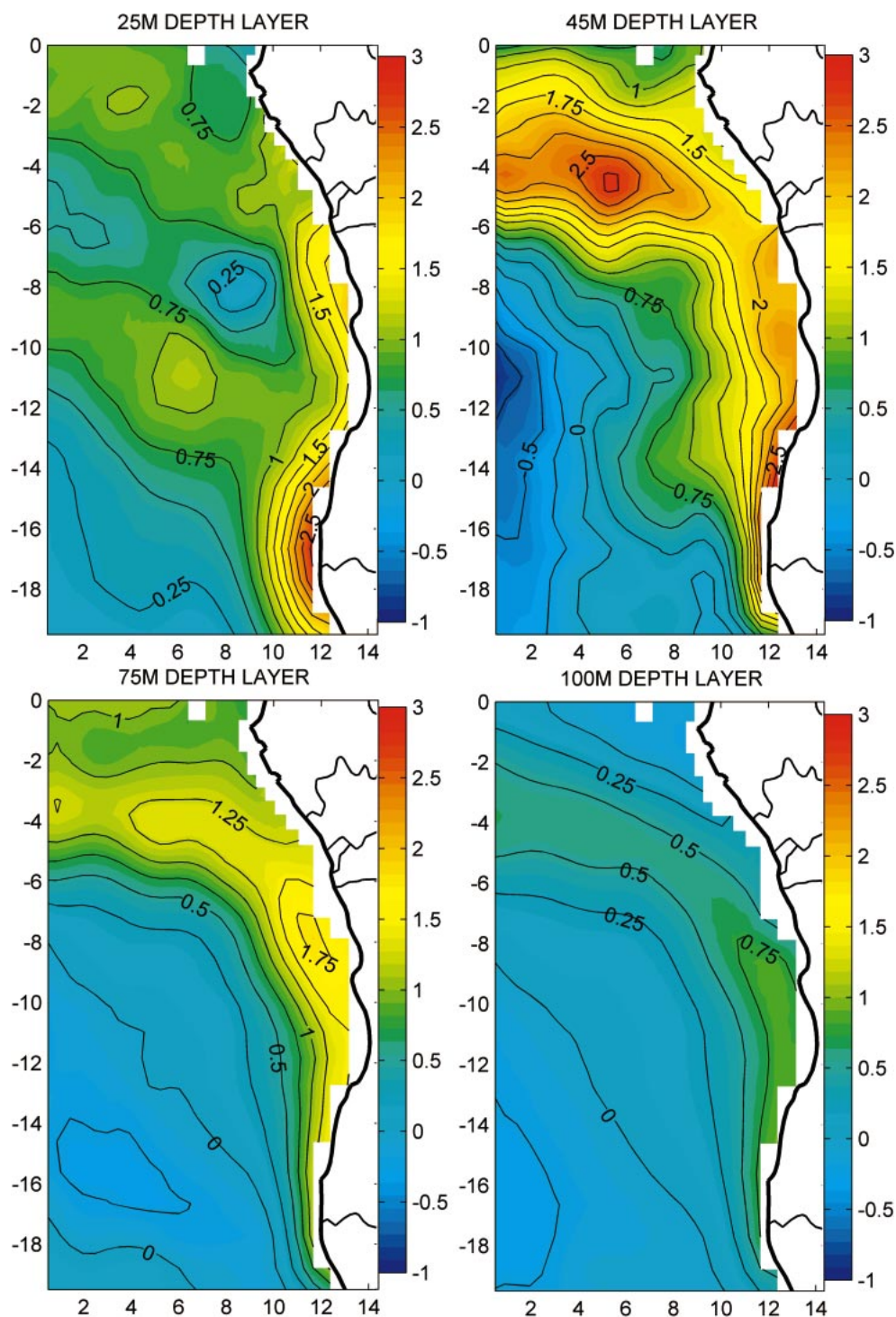
FIG. 13. Spatial coverage of model temperature anomalies at 25-, 45-, 75-, and 100-m depth levels in Apr 1995 (°C).

While little difference is observed between the 5- and the 25-m levels, the 45- and 75-m levels show rather different anomaly patterns. The 100-m level shows a similar pattern to the 75-m level, but weaker in magnitude. The model mixed layer seems to extend on av-erage to the depth of the 45-m level along the African coast, between the equator and 12°S. Hence subsurface temperatures below that depth will be less constrained by the surface boundary condition. That might partly explain the difference observed between the surface lay-
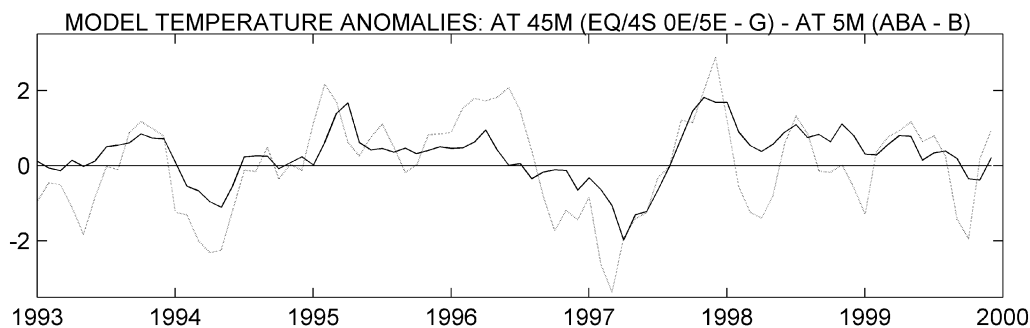
FIG. 14. Time series of model temperature anomalies at 5- and at 45-m depth layers, respectively, averaged over the ABA (black) and over an area from the equator to 4°S and from 0° to 5°E (gray) (°C).

ers and the deeper layers. Figure 14 shows two time series of model temperature anomalies at 5 and at 45 m, respectively, averaged over the ABA and over an area from the equator to 4°S and from 0° to 5°E. The maximum correlation between the signals from 1993 to 1999 is 0.69 with a 1-month lag; the signal at 45 m leads the signal at 5 m. This result indicates the consistency of anomalies between the two layers despite different spatial patterns.

Subsurface anomalies appear to affect a much larger area spreading roughly from the equator in the open ocean to slightly north of the ABA along the coast with magnitudes at least as large as the surface ones (Fig. 13). At the 100-m level, the signature of both events is still visible with a spatial coverage similar to the 45- and 75-m levels, but with much lower intensity. A similar analysis is applied to other simulated episodes; they all present quite regular patterns spreading southward from the equator at various depths. However, we note that in 1982, 1983, and 1991 maximum anomalies are observed in the 25-m layer while maximum anomalies occur at the 75-m level in 1984, 1995, 1997, and 1997/98. The first group of events peaked mainly from May to July while the other group was in phase with late summer (March/April). Once again the seasonal variation in the depth of the thermocline might explain the different expression of events. Modulation by local winds also remains a possibility, despite their weakness near the coast. Hence all episodes turn out to be large-scale events although their surface expression might be limited.

c. Origin of model anomalies

To determine the origin of simulated events and to track the anomalies across the tropical Atlantic below the surface, we have summed the monthly anomalies between the five layers for the entire domain. This procedure allows us to follow the evolution and propagation of various events whatever their depth and location. Figure 15 shows the temperature anomalies in 1995 from December to March, that is, from their first appearance in the deeper layers until they eventually reach

the ABA in the 5-m layer. It confirms the equatorial origin of the 1995 event: we note the development of subsurface warm anomalies along the equator in December (Fig. 15a), roughly 1 or 2 months before they start to outcrop in the Angola–Benguela area (Fig. 15c). The anomalies spread eastward to Africa below the surface and then propagate poleward along the coast in the ABA. The 1984 warm event shows a very similar evolution.

Anomalies created in the west-central basin spread to the African coast in 15–30 days (i.e., with a propagation rate of 1.5 to 2 m s^{-1}). The period of these waves (2 months) makes it difficult to distinguish the eastern leading "edge" of the wave since anomalies occupy almost half of the basin while they develop. Picaut and Busalacchi (2001) have given a typical phase speed of the order of 1 m s^{-1}, while Katz (1997) has suggested 2 m s^{-1}. Delecluse et al. (1994) have shown that an observed speed of 2 m s^{-1} is close to the theoretical phase speed in the Atlantic. All these characteristics suggest that the underlying mechanisms driving the major warm events along the coast of Angola and Namibia might correspond to equatorial and coastal trapped downwelling waves. Anomalies become evident at the sea surface only when and where the thermocline breaks the surface. In summer, the thermocline of the eastern tropical Atlantic Ocean only outcrops in the ABA and is part of the Angola–Benguela front. When the front is moved southward/northward under the action of an incoming downwelling/upwelling coastal wave, a warm/cold pool is produced at the surface. In both cases, anomalies seem to increase as they propagate eastward; the thermocline indeed shows a stronger vertical gradient in the eastern basin compared to the central and western parts. As a result, vertical shifts induce higher subsurface temperature anomalies near Africa.

Figure 16 depicts temperature anomaly standard deviation between the surface and the 100-m layer over the period of study. It allows a visualization of the way anomalies propagate below the surface along the coast. The depth of higher variability corresponds to the mean depth of the model thermocline and shows the path followed by the temperature anomalies. Because of the
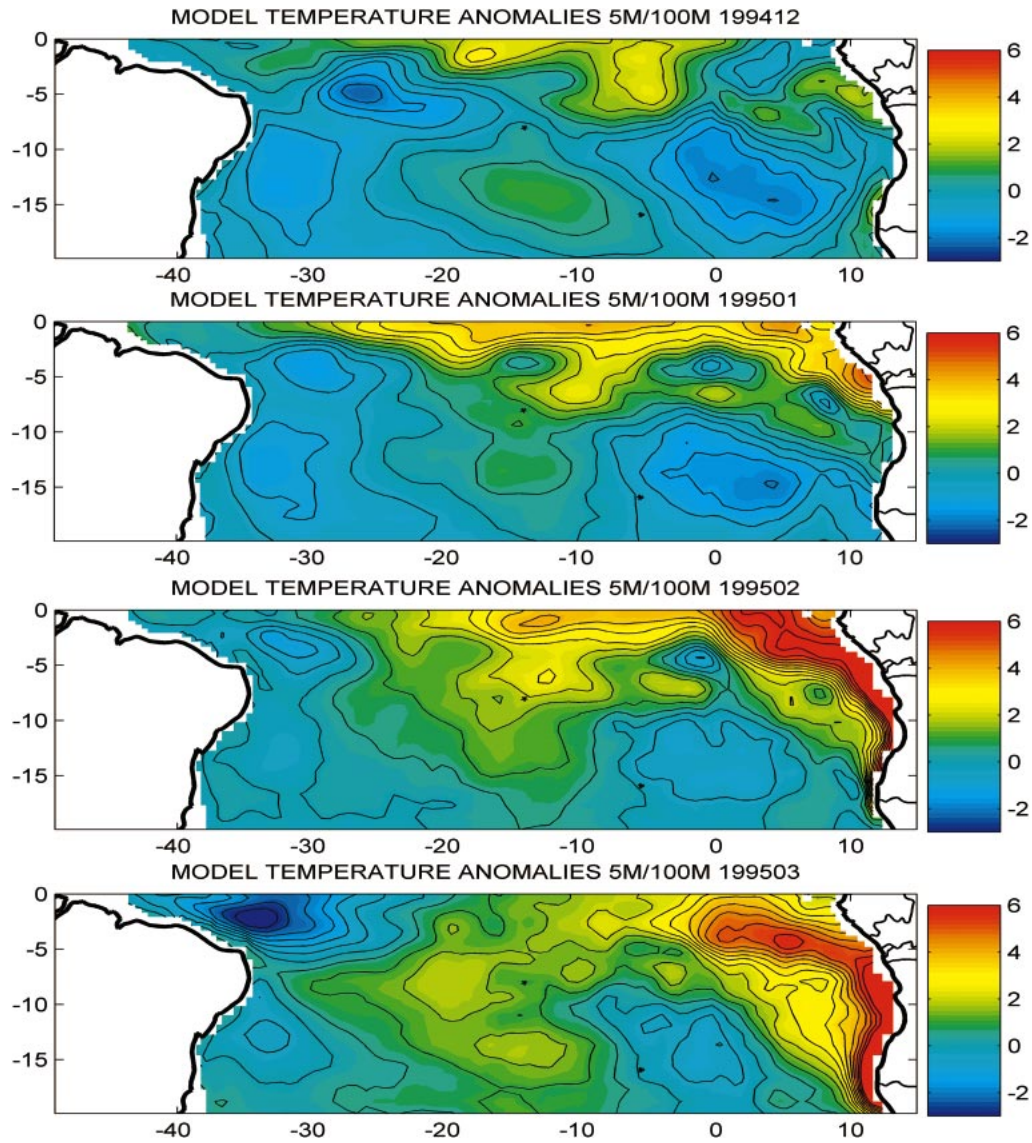
MODEL TEMPERATURE ANOMALIES 5M/100M 199412

MODEL TEMPERATURE ANOMALIES 5M/100M 199501

MODEL TEMPERATURE ANOMALIES 5M/100M 199502

MODEL TEMPERATURE ANOMALIES 5M/100M 199503

FIG. 15. Sum of model temperature anomalies between the 5-, 25-, 45-, 75-, and 100-m depth layers from Dec 1994 to Mar 1995 (°C).

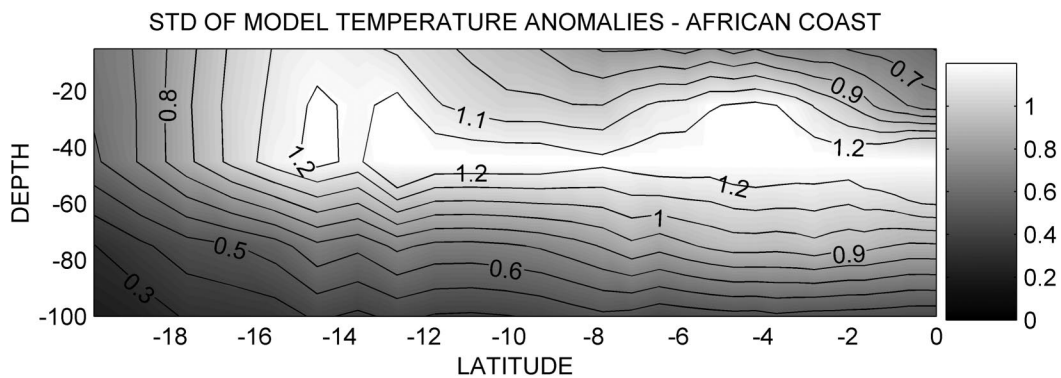STD OF MODEL TEMPERATURE ANOMALIES - AFRICAN COAST

FIG. 16. Standard deviation of model subsurface temperature anomalies along the coast of Africa (°C).

MODEL TEMPERATURE ANOMALIES (°C) - MARCH 1995

MODEL TEMPERATURE ANOMALIES (°C) - MARCH 1997
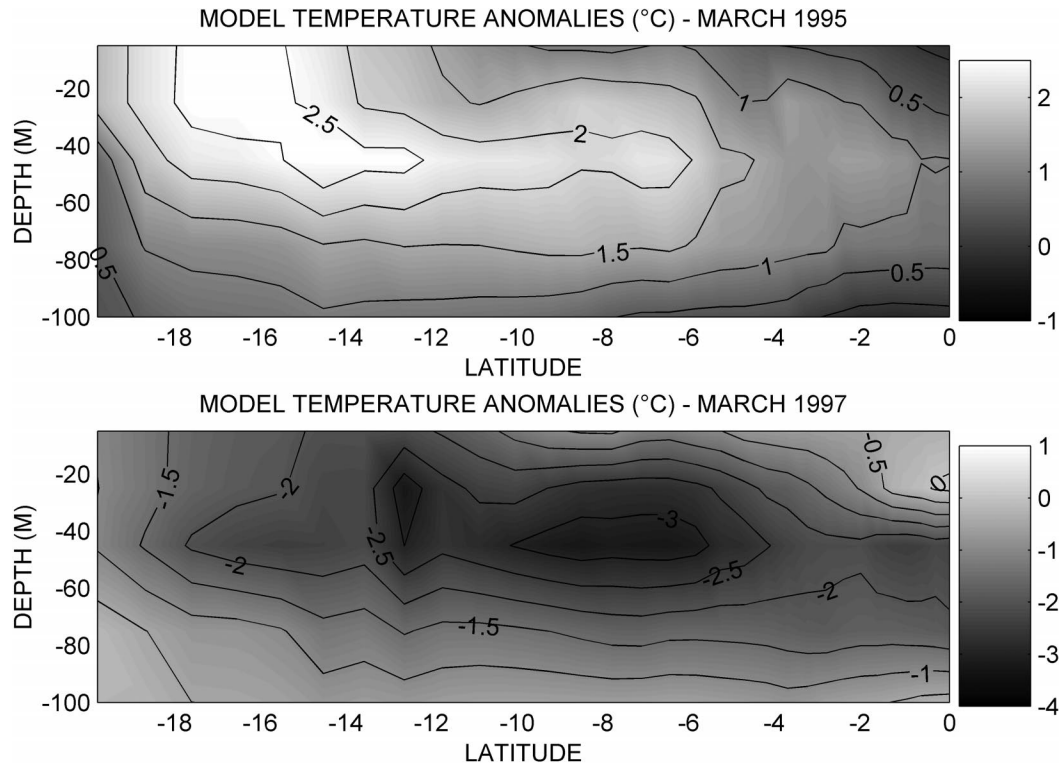

FIG. 17. Vertical section of model warm and cold temperature anomalies along the coast in (top) Mar 1995 and (bottom) Mar 1997 (°C).

strong thermal gradients associated with the thermocline, vertical and horizontal shifts of isotherms induce strong temperature anomalies visible at the surface in the ABFZ. As a result, the surface location of the anomalies will be related to the location of the ABFZ and their amplitude and spatial coverage will be partly modulated by the width of the front.

The other simulated events have also been analyzed using the same method of summing the anomalies between all layers. In all cases, warm and cold events appear to occupy a large area spreading roughly from the equator to the ABA in the eastern Atlantic Ocean. However, development and propagation of anomalies along the equator are not always as manifest as for the 1984 and 1995 events. In April 1982, we note the appearance of a cold anomaly pool at the 5- and 25-m depths in the ABA that might be related to local favorable upwelling winds. Then in June and July 1982, strong cold anomalies developed at depth along the equator and propagated eastward and then poleward along the coast to meet the ones that evolved in April. Hence this cold event could be both the result of local upwelling and wave propagation. During the 1983 cold event, anomalies start to develop along the equator in January and spread eastward in a similar way to the 1984 and 1995 events. Analyses of the 1991, 1997, and 1997/98 episodes also indicate an equatorial origin (not necessarily at the same longitude) with subsequent east-

ward and southward propagations. Kostianoy and Lutjeharms (1999) have demonstrated that the location and the intensity of the Angola–Benguela front is influenced directly by the wind stress patterns over the South Atlantic. Although these warm and cold episodes are therefore not caused by regional atmospheric disturbances over the ABA, local wind fluctuations may modify their expression at the surface as well as their impact.

Figure 17 provides two examples of warm and cold tongues spreading from the equator southward and eventually outcropping near 15°S in March 1995 (Fig. 17a) and March 1997 (Fig. 17b). It shows that the propagation process and the mechanism driving both events are very much the same. The various analyses presented earlier lead us to suggest that the mechanism driving Benguela Niños could apply to any events remotely forced in the western and central equatorial Atlantic. A few of these are the intense events with a potential impact on rainfall and biota (Benguela Niños) whereas others are minor warm episodes with a weaker impact on the environment. Conversely, extreme cold events that arise from strengthening of the trade winds could be referred to as Benguela Niñas.

7. Discussion and conclusions

A combination of various observational and model analyses at different depths suggests that, despite their

limited surface expression, warm and cold episodes along the coast of Angola and Namibia are in fact large-scale events spreading from the equator at different depths with a duration of several months.

The strong correlation between SST anomalies in the ABA and interannual zonal wind anomalies south of the equator over the western and central Atlantic basin suggests a mechanism based on equatorial and coastal trapped waves to explain the equatorial origin of most episodes. Local sea–air heat flux exchanges do not seem to precondition the sea surface in the Angola–Benguela region prior to the arrival of an event. SST anomalies become visible at the surface 1 to 2 months after the appearance of subsurface temperature anomalies at the thermocline depth. Such anomalies can be attributed to vertical shifts of the thermocline under the action of propagating equatorial Kelvin waves initially triggered by zonal wind variations. These waves are deviated poleward on approaching the African continent and temperature anomalies become more or less visible at the surface as a function of various factors like the strength of the event, the depth of the thermocline or the upwelling- or downwelling-favorable winds. Temperature anomalies start interacting with the atmosphere when and where the thermocline outcrops along the coast. Seasonal variations of the thermocline depth and shape also modulate the surface expression of the anomaly pool.

In March–April, strong SST anomalies are associated with an intense and limited pattern along the coast between 10° and 20°S while they tend to be spread from the equator southward in winter. Some cold events (which could be called Benguela Niñas) are comparable in magnitude to major warm events and their potential impact on the biota and climate needs to be investigated.

Despite the relatively rare occurrence of Benguela Niños and Niñas, warm and cold SST anomalies tend to develop regularly off Angola and Namibia. Monthly standard deviations reveal seasonality with a maximum of surface temperature variability in March/April and a minimum in September/October. Major warm events in phase with late summer are likely to give rise to Benguela Niños since they induce extremely high sea temperatures that affect the ecosystem. By interacting with the atmosphere via moisture fluxes, high SSTs may reinforce the rainfall season of southwestern Africa with sudden flooding and devastating consequences.

Sea level anomalies in the eastern equatorial basin show a strong correlation with the southern SSTA signal. The remote forcing of the SST anomalies highlights the possibility of being able to forecast future extreme events via real-time sea level and wind observations or predictive models. The development of equatorial subsurface anomalies could also be detected in advance thanks to local measurements such as the ones performed by the Pilot Research Moored Array in the Tropical Atlantic (PIRATA) array (Servain et al. 1998). However, the nonlinear response of SST anomalies in the ABA to the remote wind forcing emphasizes the need for further work to understand the way different mechanisms seem to control the development of each individual event in the tropical Atlantic basin.

REFERENCES

Blanke, B., and P. Delecluse, 1993: Variability of the tropical Atlantic Ocean simulated by a general circulation model with two different mixed layer physics. *J. Phys. Oceanogr.,* **23,** 1363–1388.

Boyd, A. J., J. Salat and M. Masó, 1987: The seasonal intrusion of relatively saline water on the shelf off northern and central Namibia: The Benguela and comparable ecosystems. *South Afr. J. Mar. Sci.,* **5,** 107–120.

Boyer, D. C., and I. Hampton, 2001: An overview of the living marine resources of Namibia. *South Afr. J. Mar. Sci.,* **23,** 5–35.

——, H. J. Boyer, I. Fossen and A. Kreiner, 2001: Changes in abundance of the northern Benguela sardine stock during the decade 1990–2000, with comments on the relative importance of fishing and the environment. *South Afr. J. Mar. Sci.,* **23,** 76–84.

Carton, J. A., and B. Huang, 1994: Warm events in the tropical Atlantic. *J. Phys. Oceanogr.,* **24,** 888–903.

Chang, P., R. Saravanan, L. Ji, and G. C. Hegerl, 2000: The effect of local sea surface temperatures on atmospheric circulation over the tropical Atlantic sector. *J. Climate,* **13,** 2195–2216.

Clarke, A. J., and S. Van Gorder, 1994: On ENSO coastal currents and sea level. *J. Phys. Oceanogr.,* **24,** 661–679.

Curtis, S., and S. Hastenrath, 1995: Forcing of anomalous sea surface temperature evolution in the tropical Atlantic during Pacific warm events. *J. Geophys. Res.,* **100,** 15 835–15 847.

Delecluse, P., J. Servain, C. Levy, K. Arpe, and L. Bengtsson, 1994: On the connection between the 1984 Atlantic warm event and the 1982–1983 ENSO. *Tellus,* **46,** 448–464.

Enfield, D. B., and J. S. Allen, 1980: On the structure and dynamics of monthly mean sea level anomalies along the Pacific coast of North and South America. *J. Phys. Oceanogr.,* **10,** 557–578.

——, and D. A. Mayer, 1997: Tropical Atlantic sea surface temperature variability and its relation to El Niño–Southern Oscillation. *J. Geophys. Res.,* **102,** 929–945.

Florenchie P., J. R. E. Lutjeharms, C. J. C. Reason, S. Masson, and M. Rouault, 2003: The source of Benguela Niños in the South Atlantic Ocean. *Geophys. Res. Lett.,* **30,** 1505, doi:10.1029/2003GL017172.

Gammelsrød, T., C. H. Bartholomae, D. C. Boyer, V. L. L. Filipe, and M. J. O'Toole, 1998: Intrusion of warm surface water along the Angolan–Namibian coast in February–March 1995: The 1995 Benguela Niño. *South Afr. J. Mar. Sci.,* **19,** 41–56.

Gilson, J. K., P. Kallberg, S. Uppala, A. Hernandez, A. Nomura, and E. Serrano, 1999: ERA-15 description. ECMWF Re-Analysis Project Report Series 1, Version 2, ECMWF, 72 pp.

Hirst, A. C., and S. Hastenrath, 1983: Atmosphere–ocean mechanisms of climate anomalies in the Angola–tropical Atlantic sector. *J. Phys. Oceanogr.,* **13,** 1146–1157.

Kalnay, E., and Coauthors, 1996: The NCEP/NCAR 40-Year Re-analysis Project. *Bull. Amer. Meteor. Soc.,* **77,** 437–471.

Katz, E. J., 1997: Waves along the equator in the Atlantic. *J. Phys. Oceanogr.,* **27,** 2536–2544.

Kostianoy, A. G., and J. R. E. Lutjeharms, 1999: Atmospheric effects in the Angola–Benguela frontal zone. *J. Geophys. Res.,* **104,** 20 962–20 970.

Lass, H. U., M. Schmidt, V. Mohrholz, and G. Nausch, 2000: Hydrographic and current measurements in the area of the Angola–Benguela front. *J. Phys. Oceanogr.,* **30,** 2589–2609.

Latif, M., and T. P. Barnett, 1995: Interactions of the tropical oceans. *J. Climate,* **8,** 952–964.

Levitus, S., 1982: *Climatological Atlas of the World Ocean.* NOAA Prof. Paper 13, 173 pp. and 17 microfiche.

Madec, G., P. Delecluse, M. Imbard, and C. Levy, 1999: OPA 8.1 Ocean General Circulation Model reference manual. Internal Report Institut Pierre-simon Laplace (IPSL), Paris, France, 91 pp.

Maes C., P. Delecluse, and G. Madec, 1998: Impact of westerly wind bursts on the warm pool of the TOGA-COARE domain in an OGCM. *Climate Dyn.,* **14,** 55–70.

Masson, S., P. Delecluse, J. P. Boulanger, and C. Menkes, 2002: A model study of the seasonal variability and formation mechanisms of barrier layer in the eastern equatorial Indian Ocean. *J. Geophys. Res.,* **107,** 8017, doi:10.1029/2001JC000832.

Meeuwis, J. M., and J. R. E. Lutjeharms, 1990: Surface thermal characteristic of the Angola–Benguela front. *South Afr. J. Mar. Sci.,* **9,** 261–279.

Mohrholz, V., M. Schmidt, and J. R. E. Lutjeharms, 2001: The hydrography and dynamics of the Angola–Benguela frontal zone and environment in April 1999. *South Afr. J. Sci.,* **97,** 199–208.

Picaut, J., 1985: Major dynamics affecting the eastern tropical Atlantic and Pacific Oceans. CalCOFI Report, Vol 26.

——, and J. Busalacchi, 2001: Tropical ocean variability. *Satellite Altimetry and Earth Sciences,* L.-L. Fu and A. Cazenave, Eds., Academic Press, 217–236.

Pizarro, O., A. J. Clarke, and S. Van Gorder, 2001: El Niño sea level and currents along the South American coast: Comparisons of observations with theory. *J. Phys. Oceanogr.,* **31,** 1891–1903.

Reason, C. J. C., R. J. Allan, J. A. Lindesay, and T. J. Ansell, 2000: ENSO and climatic signals across the Indian Ocean basin in the global context: Part I, Interannual composite patterns. *Int. J. Climatol.,* **20,** 1285–1327.

Reynolds, R. W., and T. M. Smith, 1994: Improved global sea surface temperature analyses using optimum interpolation. *J. Climate,* **7,** 929–948.

Rouault, M., P. Florenchie, N. Faucherau, and C. J. C. Reason, 2003: South East tropical Atlantic warm events and southern African rainfall. *Geophys. Res. Lett.,* **30,** 8009, doi:10.1029/2003GL014840.

Roy, C., and C. Reason, 2001: Enso-related modulation of coastal upwelling in the eastern Atlantic. *Progress in Oceanography,* Vol. 49, Pergamon, 245–255.

Ruiz-Barradas, A., J. A. Carton, and S. Nigam, 2000: Structure of interannual-to-decadal climate variability in the tropical Atlantic sector. *J. Climate,* **13,** 3285–3297.

Saravanan, R., and P. Chang, 2000: Interaction between tropical Atlantic variability and El Niño–Southern Oscillation. *J. Climate,* **13,** 2277–2292.

Servain, J., and S. Arnault, 1995: On forecasting abnormal climatic events in the tropical Atlantic Ocean. *Ann. Geophys.,* **13,** 995–1008.

——, A. J. Busalacchi, M. J. McPhaden, A. D. Moura, G. Reverdin, M. Vianna, and S. E. Zebiak, 1998: A Pilot Research Moored Array in the tropical Atlantic (PIRATA). *Bull. Amer. Meteor. Soc.,* **79,** 2019–2031.

——, I. Wainer, J. P. McCreary, and A. Dessier, 1999: Relationship between the equatorial and meridional modes of climatic variability in the tropical Atlantic. *Geophys. Res. Lett.,* **26,** 485–488.

Shannon, L. V., A. J. Boyd, G. B. Bundrit, and J. Taunton-Clark, 1986: On the existence of an El Niño-type phenomenon in the Benguela system. *J. Mar. Sci.,* **44,** 495–520.

——, J. J. Agenbag, and M. E. L. Buys, 1987: Large and mesoscale features of the Angola–Benguela front. *South Afr. J. Mar. Sci.,* **5,** 11–34.

Sutton, R. T., S. P. Jewson, and D. P. Rowell, 2000: The elements of climate variability in the tropical Atlantic region. *J. Climate,* **13,** 3261–3284.

Torrence, C., and G. P. Compo, 1998: A practical guide to wavelet analysis. *Bull. Amer. Meteor. Soc.,* **79,** 61–78.

Walker, N. D., 1987: Interannual sea surface temperature variability and associated atmospheric forcing within the Benguela system. *South Afr. J. Mar. Sci.,* **5,** 121–132.

Xie, P., and P. A. Arkin, 1998: Global monthly precipitation estimates from satellite-observed outgoing longwave radiation. *J. Climate,* **11,** 137–163.

Zebiak, S. E., 1993: Air–sea interaction in the equatorial Atlantic region. *J. Climate,* **6,** 1567–1586.